Neuroscience 569 (2025) 12–20

Contents lists available at ScienceDirect

Neuroscience

journal homepage: www.elsevier.com/locate/nsc

Diurnal dynamics of the Zbtb14 protein in the ventral hippocampus are disrupted in epileptic mice

İlke Güntan [a], Antoine Ghestem [b], Kinga Nazaruk [a], Karolina Nizińska [a], Maciej Olszewski [a], Dorota Nowicka [a], Christophe Bernard [b], Katarzyna Łukasiuk [a,*]

[a] Laboratory of Epileptogenesis, Nencki Institute of Experimental Biology of Polish Academy of Sciences, 3 Pasteur St, 02-093 Warsaw, Poland
[b] Inserm, INS, Institut de Neurosciences des Systèmes, Aix Marseille University, Marseille, France

ARTICLE INFO

Keywords:
Circadian rhythm
ZF5
Epilepsy

ABSTRACT

Our previous *in silico* data indicated an overrepresentation of the ZF5 motif in the promoters of genes in which circadian oscillations are altered in the ventral hippocampus in the pilocarpine model of temporal lobe epilepsy in mice. In this study, we test the hypothesis that the Zbtb14 protein oscillates in the hippocampus in a diurnal manner and that this oscillation is disrupted by epilepsy.

We found that Zbtb14 immunostaining is present in the cytoplasm and cell nuclei. Western blot data indicate that the cytoplasmic and nuclear levels of Zbtb14 protein oscillate, but the phase is shifted. The densities of the Zbtb14-immunopositive cells express diurnal dynamics in the ventral hilus and CA3 but not in the dorsal hilus and CA3, or the somatosensory cortex. In the pilocarpine model of epilepsy, an increase in the level of Zbtb14 protein was found at 11 PM but not at 3 PM compared to controls. Finally, *in silico* analysis revealed the presence of the ZF5 motif in the promoters of 21 out of 24 genes down-regulated by epileptiform discharges *in vitro*, many of which are involved in neuronal plasticity. Our data suggest that Zbtb14 may be involved in the diurnal dynamic of seizure regulation or brain response to seizure rhythmicity.

Introduction

The circadian rhythm is a biological oscillation of around 24 h, primarily regulated by the suprachiasmatic nucleus (SCN). This inner clock controls essential functions like the sleep-wake cycle, body temperature, hormone secretion, blood pressure, and immune functions (Markov and Goldman, 2006; Hetman et al., 2022). Although mammals have a self-regulated endogenous clock, this body clock needs to be adjusted to 24 h by the external cues called zeitgebers. Peripheral organs transmit these external cues to the SCN of the hypothalamus, and SCN neurons coordinate the peripheral clocks (Hetman et al., 2022; Schurhoff and Toborek, 2023).

Self-sustaining transcriptional and translational feedback loops within SCN and other tissues synchronize the self-regulated endogenous clock and external cues. The cycle starts with the heterodimerization of brain muscle aryl hydrocarbon receptor nuclear translocator-like 1 (BMAL1; also known as ARNTL) and circadian locomotor output cycle kaput (CLOCK) – the positive regulators, which, in turn, activate the expression of its negative regulators, cryptochrome-1/2 (CRY1,2) and period-1/2/3 (PER1,2,3), among other downstream circadian rhythm modulators like RORα, REV-ERBα, and REV-ERBβ (Hastings et al., 2018).

Circadian rhythms are modified in numerous neurological disorders (Rijo-Ferreira and Takahashi, 2019; Hetman et al., 2022; Lane et al., 2023), including epilepsy (Debski et al., 2020). Conversely, disrupting the circadian machinery may lead to epilepsy (Li et al., 2017). Most, if not all, patients with epilepsy present a circadian regulation of their seizures (Karoly et al., 2021), a property also observed in experimental models (Quigg et al., 1998; Baud et al., 2019). This oscillatory pattern of seizures may be linked to altered circadian rhythms (Bernard, 2021).

In epileptogenic regions, like the hippocampus, the circadian rhythmicity is altered. The expression of seven core genes (BMAL1, CLOCK, CRY1/2, and PER1/2/3) is perturbed in the hippocampus in an experimental model of temporal lobe epilepsy (Matos et al., 2018). We have previously shown that in both control and experimental epilepsy conditions, the levels of a large number of transcripts and proteins oscillate in a circadian manner (Debski et al., 2020). In the study, we reported diurnal oscillations in over 1200 transcripts in the control and

* Corresponding author.
E-mail address: k.lukasiuk@nencki.edu.pl (K. Łukasiuk).

https://doi.org/10.1016/j.neuroscience.2025.01.039
Received 24 July 2024; Accepted 17 January 2025
Available online 25 January 2025

over 1600 in the epileptic ventral hippocampus. We observed varied alterations in gene expression signatures in epileptic animals. We identified genes that gained a circadian oscillatory pattern, others lost theirs, and a subset of genes had alterations in their amplitude or had a shift of several hours in their oscillations (Debski et al., 2020). The origin of these alterations is not known. The functional enrichment analysis of the promoters of the transcripts grouped in clusters with similar expression patterns revealed several transcription factor binding motifs as putative regulators of the expression of genes with diurnal oscillations altered in epilepsy. The ZF5 motif appeared for several clusters. (Debski et al., 2020).

The Zbtb14 protein (formerly also known as ZNF478, ZFP161, ZFP5, ZF5) binds to the ZF5 motif on gene promoters and is expressed in the brain (https://www.genecards.org/cgi-bin/carddisp.pl?gene=ZBTB14) (Yokoro et al., 1998; Obata et al., 1999). Zbtb14 protein is poorly characterized. It contains five C_2H_2 (Krüppel-type) zinc fingers on its C-terminus and POZ/BTB (Broad-complex, Tramtrack and Bric-a-brac/Poxvirus and Zinc-finger) domain in its N-terminus (Numoto et al., 1993). It is expressed in several human and mouse tissues, including the testis, liver, brain, muscle, thymus, and spleen (Yokoro et al., 1998). Zbtb14 can act as a transcriptional repressor, e.g., of the human fragile X-mental retardation 1 (FMR1) gene and leukemia inhibitory factor (Lif), or as a transcriptional activator, e.g., of the human dopamine transporter (hDAT) and interleukin 6 (Il6) (Lee et al., 2004; Orlov et al., 2007; Nylén et al., 2018).

In this study, we test the hypothesis that the Zbtb14 protein oscillates in the hippocampus in a circadian manner and that this oscillation is disrupted by epilepsy.

Materials and methods

Animals, time-pointed tissue collection, and epilepsy induction

All animal procedures were conducted on FVB male mice following European Council Directive 2010/63/EU and ARRIVE guidelines.

Naïve animals for time-pointed tissue collection were obtained from the Nencki Institute Animal Facility and performed at the Nencki Institute of Experimental Biology (Polish Academy of Sciences, Warsaw, Poland). All experiments on control and epileptic animals were performed at INSERM, INS, Institut de Neurosciences des Systèmes, Aix Marseille University, Marseille, France, following INSERM procedures on FVB adult male mice as described in Debski et al. (Debski et al., 2020).

Mice were housed in a controlled environment (7:30 am–7:30 pm, light on/off) with water and food available *ad libitum*. During the dark phase, a red light was used while handling animals. Any other light source was off to ensure the circadian rhythm was unaffected. The animals were kept together in groups (max. six animals per cage), and cardboard tunnels and snacks enriched their environment. In addition, the same researchers took care of the animals to reduce the external stressors.

For time-pointed tissue collection, animals aged of 16th and 19th weeks were anesthetized with isoflurane at 11 am, 3 pm, 7 pm, 11 pm, 3 am, and 7 am. The brain's left hemispheres were fresh-frozen on dry ice for immunofluorescent staining and stored at −80 °C. The right hippocampi were removed from the hemispheres and immediately used to extract nuclear and cytoplasmic protein extracts.

To induce epilepsy, 2-month-old FVB mice were injected with methylscopolamine [1 mg/kg, intraperitoneally (ip)] 30 min before the pilocarpine injections. After that, pilocarpine was repeatedly injected (100 mg/kg, ip) every 20 min until status epilepticus (SE) was observed. After 90 min of SE, we injected diazepam (10 mg/kg, ip) to stop SE. All mice then received 0.5 ml of NaCl (0.9 %) subcutaneously and again in the evening. If required, mice were fed using a syringe during the following days. Control mice had the same treatment but were only injected with intraperitoneal NaCl (0.9 %). Three months after SE mice were anesthetized with isoflurane in the animal facility and were sacrificed at the same time points: 3 pm and 11 pm. The hippocampus was removed in modified ice-cold artificial cerebrospinal fluid (ACSF). Both hippocampi from the same animal were quickly frozen and stored together at −80 °C.

Immunofluorescent double staining

Sagittal sections (20 μm) were cut with a cryostat (Leica CM1860), collected on poly-L-lysine-coated glass microscope slides, and stored at −80 °C. Sections were fixed in ice-cold acetone for 10 min. Slides were washed in 0.5 % Triton X-100 (Sigma) in PBS (PBST) thrice for 5 min. Unspecific binding was blocked by 90 min of incubation with 5 % normal goat serum (Vector, #S-1000) at room temperature. Next, the sections were incubated overnight in a humid chamber with rabbit anti-ZBTB14 antibody (1:100; Atlas Antibodies, #HPA050758) diluted in PBST at 4 °C. The following day, the slides were washed in PBST three times for 5 min and incubated for 2 h with goat anti-rabbit IgG antibody (H + L), biotinylated (1:200; Vector, BA-1000) diluted in PBST at room temperature. This was followed by washing and incubation for 20 min with fluorescein avidin D, FITC (1:100; Vector, A-2001) at room temperature. After washing, the sections were blocked at room temperature for 90 min of incubation with 2 % normal donkey serum (Jackson ImmunoResearch, #017–000-121). Next, the sections were incubated overnight in a humid chamber with mouse anti-NeuN antibody, clone A60 (1:1000; Sigma-Aldrich, #MAB377) diluted in PBST at 4 °C. The following day, the slides were washed and incubated for 2 h with donkey anti-mouse IgG (H + L) highly cross-adsorbed secondary antibody, Alexa Fluor 568 (1:2000; Invitrogen, #A-10037) diluted in PBST at room temperature. Nuclei were stained with Hoechst dye (1:2000; Sigma-Aldrich). Finally, the slides were washed in PBS thrice for 5 min and rinsed in cold tap water. They were dried overnight and cover-slipped with Vectashield Mounting Medium (Vector, #H-1000) the next day, stored at 4 °C. The omission of primary antibodies verified the specificity of antibodies.

Quantification of the density of Zbtb14-positive cells

Sections were viewed with a Nikon Eclipse 80i microscope, and images were captured using a CCD camera (Evolution VF; MediaCybernetics) with a Nikon 10/0.30 DIC L/N1 or 20/0.50 DIC M/N2 objective. Images were acquired for each area examined using different filters for Alexa Flour 568, FITC, and Hoechst and elaborated with Image-ProPlus, version 5.0 for Windows (MediaCybernetics). The sections from the 2.28 – 2.40 mm lateral level from the midline were visually inspected under the microscope. All images were collected using the same exposure time, and then corresponding pictures were superimposed to visualize the co-localization of the NeuN-stained neurons with the Zbtb14 immunofluorescence. Data were collected from a manually delineated area covering the hilus (separately ventral and dorsal areas), CA3 area (averaged from two separate frames covering CA3a), and somatosensory cortex (−2 from bregma, same sections as for hilus). The hilus was distinguished according to Amaral et al., (Amaral et al., 2007). For the cortex, data was calculated from a 200 μm-wide profile of the somatosensory cortex. The profile was divided into cortical layers II/III, IV, V, and VI according to Hoechst staining, which was evaluated separately. The Zbtb14-positive cells were manually tagged and counted within the area of interest. NeuN/Zbtb14 double-stained cells were also recorded in the ventral hilus. Only the cells with well-visible nucleoli (visualized with Hoechst staining) were included in the analysis. The expression for each marker was analyzed as the number of positive cells per mm^2. Figures were prepared using Adobe Photoshop CS2 and Corel Draw X4. Brightness and contrast were adjusted to regain the natural appearance of the sections.

Protein extraction and western blot

The right hippocampi from the time-pointed tissue collection were used for nuclear and cytoplasmic protein extraction. The nuclear and cytoplasmic protein extraction was performed using NE-PER™ Nuclear and Cytoplasmic Extraction Reagents kit (Thermo Scientific, #78833) according to the manufacturer's instructions. The concentration of the protein extracts was measured using Protein Assay Dye Reagent (Bio-Rad, #5000006).

The fresh-frozen brain tissue from control and epileptic animals was homogenized with a handheld rotor–stator homogenizer (QIAGEN, TissueRuptor II) in a lysis buffer that contains 0.5 % Triton X-100, 50 mM potassium chloride, 50 mM PIPES, 2 mM magnesium chloride, and 20 mM EGTA with the addition of 0.1 mM phenylmethylsulfonyl fluoride, 1 mM dithiothreitol, 1X proteinase inhibitor cocktail (Roche, #11697498001). The tissue lysate was frozen for 20 min at −20 °C. After thawing, the samples were centrifuged at 4 °C, 11000 rpm, for 20 min; the supernatant was transferred into a clean tube and stored at −80 °C. The concentration of the protein isolates was measured using Protein Assay Dye Reagent (BioRad, #5000006). 20 µg of protein for cytoplasmic extracts from naïve animals, control and epileptic animal total protein isolates, and 4 µg nuclear protein samples were loaded for Western Blot. For each gel, a 7 ul protein ladder was loaded (10 to 180 kDa) [molecular weight range in kDa (kilodalton)] (Thermo Fisher Scientific, Waltham, MA, USA, #26616). Protein isolates were separated via Tris-glycine sodium dodecyl sulfate–polyacrylamide gel electrophoresis (SDS-PAGE) and transferred to a nitrocellulose blotting membrane (Cytiva, #10600002). The membranes were blocked in 5 % nonfat milk in TBS-T (150 mM NaCl, 10 mM Tris, and 0.1 % Tween20, pH 8.0) for 1 h at room temperature. Next, they were incubated overnight in rabbit anti-ZBTB14 (1:1000; Atlas Antibodies, #HPA050758) diluted in TBS-T at 4 °C. After washing with TBS-T, the membranes were incubated for 2 h in goat anti-rabbit IgG antibody, peroxidase-conjugated (1:10000; Sigma-Aldrich, #AP132P) diluted in TBS-T at room temperature. The signal was detected using ECL Prime Western Blotting System (Cytiva, #RPN2232) according to the manufacturer's instructions. The signal was captured on an X-ray film with an automatic film processor. After stripping (93 mM glycine, 69 mM sodium dodecyl sulfate, pH 3.0), the membranes were re-probed with anti-β-actin – peroxidase antibody, mouse monoclonal (1:240000; Sigma-Aldrich, #A3854) diluted in TBS-T. X-ray films were scanned using GS-900 Calibrated Densitometer (BioRad), and optical density was measured using Image Lab Software version 5.2.1. GraphPad Prism version 5.01 was used for statistical analysis.

In vitro model of epileptiform discharges

Embryos at 18 days post-fertilization (E18) were used to establish primary cultures of cortical neurons (Xu et al., 2012). Isolated embryos were decapitated, the hemispheres were isolated in a chilled HBSS buffer (Thermo Fisher, #14170-088), and incubated at 37 °C for 15 min with HBSS buffer containing 0.2 % Trypsin (Thermo Fisher, #27250-0180) and 0.15 mg/ml DNase (Sigma-Aldrich, #DN-25). The solution was removed, and warm 10 % FBS (Thermo Fisher, #10106-151) diluted in HBSS was added. After washing the tissue twice with fresh, warm HBSS without FBS, 2 ml of warm medium containing 1x B-27, 10 % FBS, 10 mg/ml Gentamicin, 0.5 mM Glutamax in Neurobasal Medium was added, and then the tissue was pipetted several times. The number and viability of cells were measured in 0.4 % Trypan Blue using a Neubauer chamber (Marienfeld). Two hundred thousand cells per well were seeded into a 12-well plate pre-coated with poly-D-lysine (5 µg/ml) in 0.1 M borate buffer (Sigma-Aldrich, #P7280). Cultures were grown in an incubator at 37 °C and 5 % CO_2. Half of the medium was exchanged for FBS serum-free medium (1x B-27, 10 mg/ml Gentamicin, 0.5 Mm Glutamax in Neurobasal Medium) on days 2 and 6.

Epileptiform discharges were induced *in vitro* as described by Jiang et al., (Jiang et al., 2010) with modifications (Nizińska K et al., submitted). Briefly, cultures were incubated for 3 h in pBRS buffer without magnesium (145 mM NaCl, 2.5 mM KCl, 10 mM HEPES, 2 mM $CaCl_2$, 10 mM glucose, 0.002 mM glycine, pH = 7.3). The control cultures were incubated in pBRS buffer with magnesium (145 mM NaCl, 2.5 mM KCl, 10 mM HEPES, 2 mM $CaCl_2$, 10 mM glucose, 0.002 mM glycine, 1 mM $MgCl_2$, pH = 7.3). At the end of the incubation, the pBRS buffer was replaced with a fresh, warmed, serum-free culture medium (37 °C). Material for RNA-seq studies was collected 24 h after induction of epileptiform discharges.

RNA isolation and new-generation sequencing

RNA using Qiazole (Qiagen, #79306) and RNeasy Mini Kit (Qiagen, #74104) according to the manufacturer's instructions. The RNA was measured on a Nanodrop Spectrophotometer (DeNovix, #DS-11 Spectrophotometer) at λ = 260 nm and 280 nm. The isolated RNA was stored at −80 °C. RNAseq libraries were prepared by KAPA Stranded mRNA Sample Preparation Kit according to the manufacturer's protocol (Kapa Biosystems, MA, USA) as previously described (Grabowska et al., 2022). Transcriptomic data analysis was done as follows: fastq files were aligned to the rn6 rat reference genome with the STAR program (Dobin et al., 2013), and reads were counted to genes using the feature Counts algorithm (Liao et al., 2014). Gene counts were normalized with the FPKM method, and differential analysis was performed by DESeq2 (Love et al., 2014). Genes were considered to be differentially expressed with adjusted p-value < 0.05.

Using g: Profiler (https://biit.cs.ut.ee/gprofiler/gost), we analyzed the overrepresentation of transcription factor binding motifs in groups of genes.

Data are deposited at the NCBI GEO repository with the submission number GSE227084 (https://www.ncbi.nlm.nih.gov/geo/query/acc.cgi?acc=GSE227084).

Statistic methodology

Relative levels of Zbtb14 protein in the cytoplasm and nuclei are expressed as multiples of relative ratios at 11AM. The relative ratios of Zbtb14 to β-actin are represented as the mean ± SEM (n = 6). The difference between time points was evaluated with one-way ANOVA with Tukey's multiple comparison post hoc test. Zbtb14 protein-positive cell densities in the dorsal and ventral hilus were analyzed by one-way ANOVA with Tukey's multiple comparison post hoc test (n = 4 to 6). Zbtb14 protein expression in the hippocampus in pilocarpine-induced epilepsy was evaluated using one-way ANOVA with Bonferroni's multiple comparison post hoc test.

Results

Localization of Zbtb14 immunostaining

Cellular localization of the Zbtb14 protein in the ventral hippocampus and somatosensory cortex of control mice was evaluated by immunohistochemistry. We focused on the ventral hippocampus because this is the most epileptogenic zone in patients and animal models (Wyeth et al., 2020; Buckmaster et al., 2022). Zbtb14 immunostaining was observed in the cytoplasm and cell nuclei. Moreover, the Zbtb14 protein-expressing cells were also NeuN-positive, indicating neuronal localization of the Zbtb14 expression (Fig. 1).

The diurnal dynamics of Zbtb14 protein levels in the cytoplasmic and nuclear compartments

Zbtb14 protein levels through the diurnal cycle were evaluated separately in the cytoplasmic and nuclear extracts. Data are presented as multiples of the first time point after the light was turned on, i.e., 11 AM

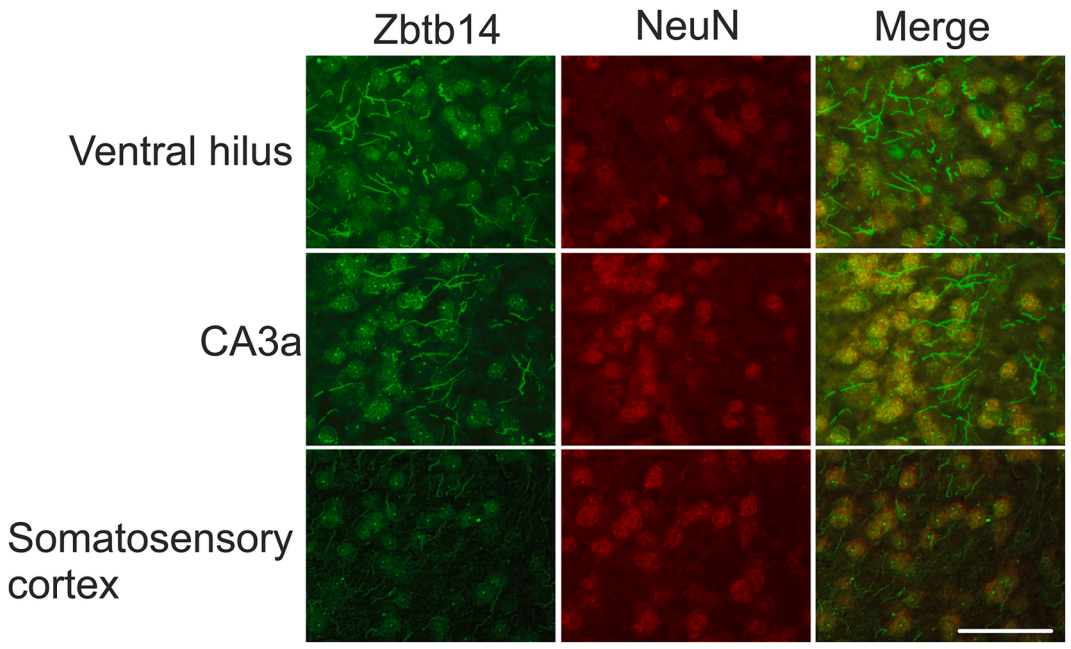

Fig. 1. Cellular localization of Zbtb14 and NeuN at 3 AM in the hippocampus and the somatosensory cortex. Representative images from the ventral hilus, CA3a of the hippocampus, and layer VI of the somatosensory cortex of naive mice. Scale bar: 50 μm.

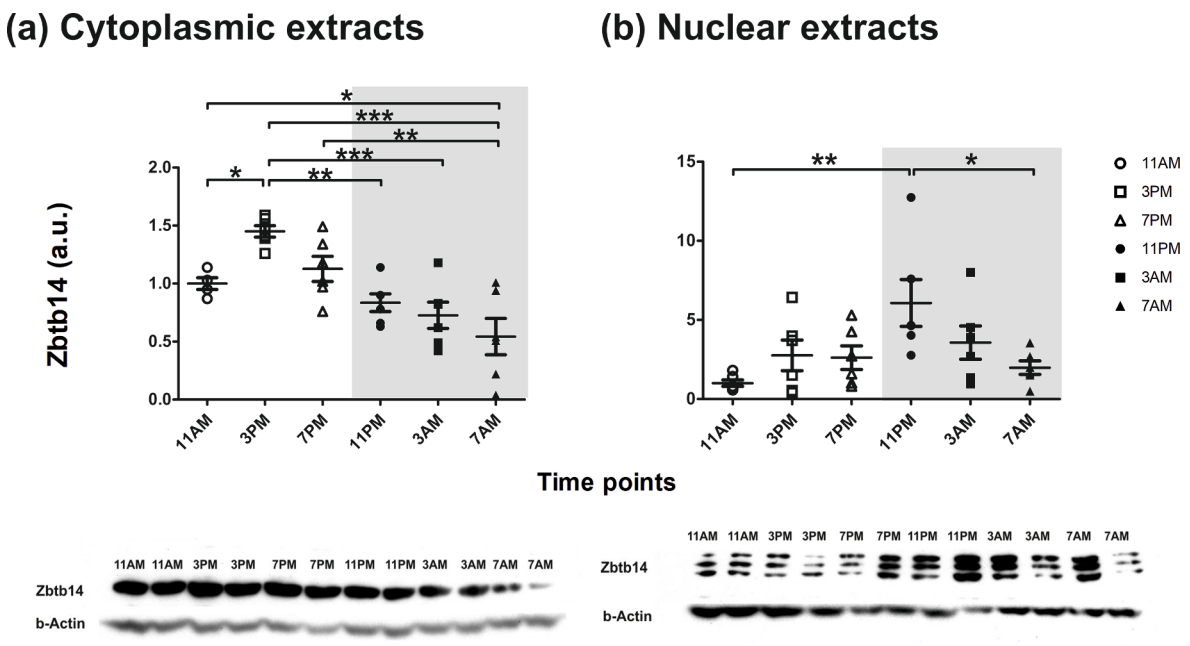

Fig. 2. Relative levels of Zbtb14 protein in the cytoplasm and nuclei in the hippocampus throughout the circadian cycle. The data are expressed as multiples of the relative ratios at 11 AM in the cytoplasmic **(a)** or nuclear **(b)** extracts, respectively. The relative ratios of Zbtb14 to β-actin are represented as the mean ± SEM (n = 6, *p < 0.05, **p < 0.01, ***p < 0.001, one-way ANOVA with Tukey's multiple comparison post hoc test).

(Fig. 2). In the cytoplasm, the Zbtb14 protein level increased by 1.45 ± 0.05 at 3 PM compared to 11 AM ($p < 0.05$) and then gradually decreased to 1.13 ± 0.11 at 7 PM, 0.84 ± 0.08 at 11 PM ($p < 0.01$ compared to 3 PM), 0.73 ± 0.11 at 3 AM ($p < 0.001$ compared to 3 PM), and 0.54 ± 0.16 at 7 AM ($p < 0.05$ compared to 11 AM; $p < 0.001$ compared to 3 PM, and $p < 0.01$ compared to 7 PM). No significant differences were observed in the Zbtb14 protein level in the cytoplasm during the light-off phase.

Different dynamics were observed in Zbtb14 protein levels in the nuclear extracts. During the light-on phase, the level of Zbtb14 was not different from the level at 11 AM and was 2.76 ± 0.96 at 3 PM, and 2.61 ± 0.75 fold greater at 7 PM. At 11 PM, the level of Zbtb14 was 6.07 ± 1.48 fold greater than at 11 AM ($p < 0.01$). Then, the levels gradually decreased to 3.57 ± 1.05 at 3 AM and then to 1.98 ± 0.43 at 7 AM, significantly lower than at 11 PM ($p < 0.05$).

The diurnal dynamics of the density of Zbtb14-expressing cells

We then assessed the temporal pattern of the density of Zbtb14-expressing cells in the dorsal and ventral hilus, dorsal and ventral

CA3a of the hippocampus, and individual layers of the somatosensory cortex using immunostaining (Fig. 3). Representative images of the Zbtb14 staining pattern at 3 PM, 11 PM, and 3 AM are presented in Fig. 4.

The density of Zbtb14-positive cells showed no significant change at the observed time points in the dorsal hilus, dorsal CA3a, and the somatosensory cortex (Fig. 3 a, c, e-h). On the contrary, the density of Zbtb14-positive cells revealed significant differences throughout the diurnal cycle in the ventral hilus and CA3a areas (Fig. 3 b and d). The mean density of Zbtb14-positive cells in the ventral hilus at 11 AM, the first time point after the light was on, was 43.01 ± 4.88 cells/mm^2. It increased significantly at 3 PM to 81.85 ± 8.88 cells/mm^2 ($p < 0.01$ compared to 11 AM). Then, it decreased steadily, reaching 64.35 ± 2.22 cells/mm^2 at 7 PM and 28.68 ± 5.31 cells/mm^2 at 11 PM ($p < 0.001$ compared to 3 PM and $p < 0.01$ compared to 7 PM). Next, the density of Zbtb14-positive cells increased again and was 73.74 ± 8.25 cells/mm^2 at 3 AM ($p < 0.001$ compared to 11 PM; $p < 0.05$ compared to 11 AM, and 86.40 ± 4.14 at 7 AM ($p < 0.001$ compared to 11 PM; $p < 0.001$ higher compared to 11 AM).

The mean density of Zbtb14-positive cells in the ventral CA3a at 11 AM was 191.6 ± 8.91 cells/mm^2 and remained unchanged at 3 PM, 188.1 ± 5.73 cells/mm^2, and at 7 PM, 218.9 ± 10.26 cells/mm^2. During the light-off phase, Zbtb14-positive cell density first dropped down to 141.4 ± 8.83 cells/mm^2 at 11 PM ($p < 0.001$ compared to 7 PM, $p < 0.01$ compared to 11 AM and 3 PM) and then started to increase to 153.0 ± 5.65 cells/mm^2 at 3 AM ($p < 0.001$ compared to 7 PM, $p < 0.05$ compared to 11 AM and 3 PM), and to 192.7 ± 7.47 cells/mm^2 at 7 AM ($p < 0.01$ compared to 11 PM, $p < 0.05$ compared to 3 AM), which was not different from the density at 11 AM.

The data suggest that diurnal rhythm modulates Zbtb14 protein expression in the ventral hippocampus but not in the dorsal and somatosensory cortex.

Overrepresentation of ZF5 motif in promoters of genes downregulated in the in vitro model of epileptiform discharges

A transcriptomics data set containing gene expression profiles 24 h after induction of epileptiform discharges in neurons *in vitro* was used to evaluate the frequency of the ZF5 motif in genes whose expression was altered. *In silico* analysis revealed the overrepresentation of the ZF5 motif in the promoters of genes affected. The ZF5 motif was present only in promoters of down-regulated genes and was detected in promoters of 21 out of 24 down-regulated genes, which is significantly different ($p_{adj} = 7.233 \times 10^{-4}$) than expected (Table 1).

Zbtb14 protein expression in an in vivo model of a temporal lobe epilepsy

The expression of Zbtb14 in the hippocampus was evaluated in the pilocarpine model of epilepsy in mice. Tissues were collected at two selected time points: 3 PM and 11 PM (Fig. 5). The selection of time points based on the mRNA differences of the transcriptome of control vs. epileptic mice observed by Debski et al., (Debski et al., 2020). No difference was observed in protein levels between control and epileptic animals at 3 PM (1.64 ± 0.62 vs. 2.84 ± 0.61 a.u., respectively). However, at 11 PM, the expression of Zbtb14 was significantly higher in epileptic animals than in controls (19.95 ± 2.24 vs. 3.73 ± 1.16 a.u. respectively, $p < 0.001$). Expression of Zbtb14 in epileptic animals was significantly higher at 11 PM compared to 3 PM ($p < 0.001$).

Discussion

Our work revealed that: (i) the Zbtb14 protein is expressed in neurons in the mouse brain; (ii) Zbtb14 protein levels oscillate through the diurnal cycle in the ventral hippocampus but not in the dorsal hippocampus; (iii) the oscillation of the Zbtb14 protein occurs in both the cytoplasm and nucleus but in a different temporal pattern; (iv) the diurnal dynamics of the Zbtb14 protein are perturbed in epilepsy in an *in vivo* model of epilepsy; (v) numerous genes that are downregulated in the *in vitro* model of epileptiform discharges have a ZF5 motif in their promoters.

Our data indicate that ZBTB14 is exclusively expressed in neurons. In the hippocampus, it is found in both the cell's cytosol and nucleus. Furthermore, the expression of the Zbtb14 protein follows distinct circadian patterns in these two cellular compartments. The highest Zbtb14 protein level was observed in the cytoplasm at 3 pm, and the lowest levels were observed during the light-off phase. In the nucleus, the Zbtb14 level peaks at 11 pm and then gradually decreases during the dark period. This suggests that the transport of the Zbtb14 protein into the nucleus might preferentially occur at the beginning of the dark period. As a transcription factor, being in the nucleus is essential for the role of the Zbtb14 protein; regulating its transport from the cytoplasm to the nucleus might be a way to control its function in a time-dependent manner. Our data show that the Zbtb14 protein can cross the nuclear envelope, but there is no literature on how the Zbtb14 protein is being shuttled into the nucleus. The UniProt database suggests a domain between 50 and 66 amino acids could act as a nuclear localisation signal (NLS) of the Zbtb14 protein (https://www.uniprot.org/uniprotkb/O43829/entry#family_and_domains). Alternatively, as a small protein with a predicted molecular weight of 51 kDa and an observed molecular weight of ~ 55 kDa, Zbtb14 could be translocated to the nucleus spontaneously (Tamanini et al., 2005). Transportation of the Zbtb14 protein might be controlled at the level of translation, post-translational modifications, time-controlled accumulation at the nuclear membrane border and/or protein degradation, similar to other Zbtb protein (Tamaru et al., 2003, Tamanini et al., 2005) The precisely controlled cytoplasm-nucleus trafficking may control the function of Zbtb14 as a transcription factor.

Overrepresentation of the ZF5 motif in the promoters of clock-controlled genes in the heart, liver, muscles, suprachiasmatic nucleus, and the ventral hippocampus has already been suggested based on *in silico* analysis (Bozek et al., 2009; Debski et al., 2020). The notion that densities of Zbtb14-positive cells oscillate during the diurnal cycle only in the ventral and not in the dorsal hippocampus is attractive regarding the hippocampal heterogeneity over the longitudinal axis. The ventral hippocampus differs in connectivity, gene expression pattern, neurochemical pattern, and function from the dorsal hippocampus in rodents (O'Leary and Cryan, 2014; Bienkowski et al., 2018; Brancati et al., 2021; Lothmann et al., 2021). The oscillation of Zbtb14, and potentially its targets, in the ventral hippocampus may play a role in the diurnal regulation of the functions specific to the ventral hippocampus. This hypothesis remains to be tested.

The ventral hippocampus is a primary epileptogenic zone in pilocarpine-induced epilepsy in rodents and also in the anterior hippocampus in humans (Wyeth et al., 2020; Buckmaster et al., 2022). Interestingly, we have found that the circadian dynamics of Zbtb14 are altered in epileptic animals. At 11 pm, epileptic animals had almost six times higher levels of Zbtb14 protein in whole tissue extracts than control animals. The 11 pm time-point is the peak expression time-point of the Zbtb14 protein in nuclear extracts. The higher expression of the Zbtb14 protein may be related to the higher accessibility of Zbtb14 in the nucleus for transcriptional regulation. This would presumably result in the altered expression of the Zbtb14 target genes.

The analysis of the effect of the epileptiform discharges *in vitro* revealed that 21 out of 24 downregulated genes contain the ZF5 motif in their promoters. Interestingly, 11 of those are expressed in the mouse brain: Adamts15, Bola1, Camkk1, Grik1, Kcnab2, Lrrc24, Ppp1r3e, Sh3rf3, Slc7a4, Synpr, and 1700030J22Rik according to the Allen Brain Atlas (https://mouse.brain-map.org/). An additional six genes were found to be detected in the mammalian brain according to a PubMed search: Adamts8 (Dunn et al., 2006; Rossier et al., 2015) Hcrtr1 (Scott et al., 2011, Li et al., 2018), Inha (Fujimura et al., 1999), Polr3k (Lata et al., 2021), Rtl6 (Irie et al., 2022), and Rxrg (McCullough et al., 2018).

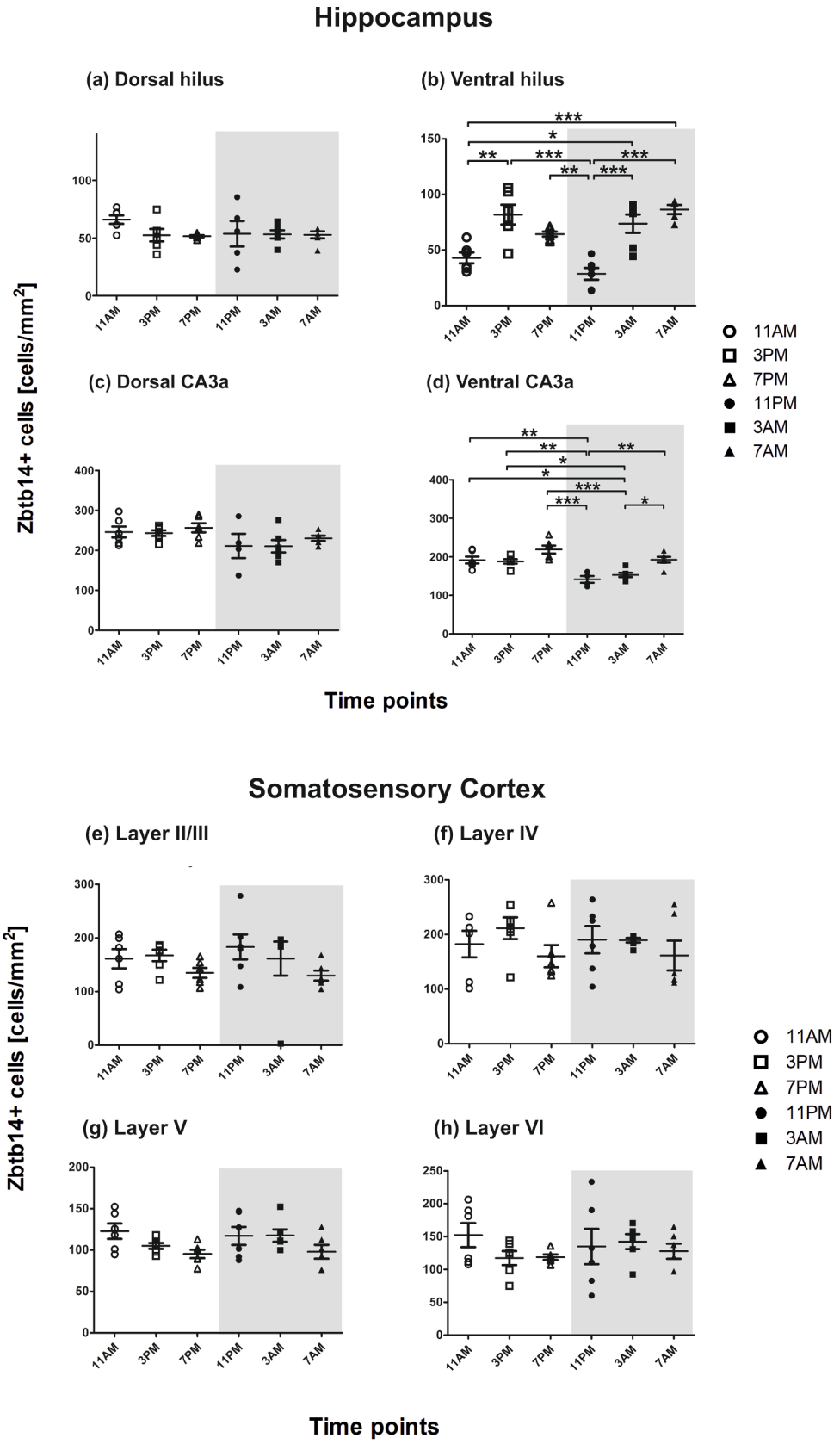

Fig. 3. Zbtb14 protein-positive cell densities in the dorsal and ventral hilus and CA3a of the hippocampus and the somatosensory cortex. The density of Zbtb14-positive cells was counted in **(a)** dorsal hilus (n = 5 for the time-point 11 PM, and n = 6 for the other time points), **(b)** ventral hilus (n = 5 for the time-point 7 AM, and n = 6 for the other time points), **(c)** dorsal CA3a (n = 4 for the time-point 11 PM, and n = 6 for the other time points), **(d)** ventral CA3a (n = 4 for the time-point 11 PM, and n = 6 for the other time points), **(e)** layer II/ III (n = 6 per time-point), **(f)** layer IV (n = 6 per time-point), **(g)** layer V (n = 6 per time-point), and **(h)**

layer VI (n = 6 per time-point). Values are represented as the mean number of cells/mm^2 ± SEM. Data are analyzed by one-way ANOVA with Tukey's multiple comparison post hoc test (*p < 0.05, **p < 0.01, ***p < 0.001).

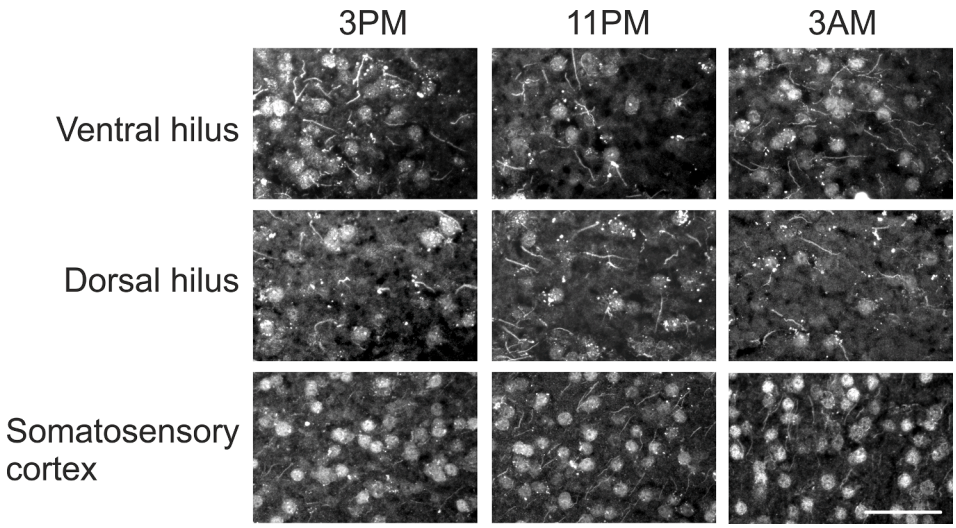

Fig. 4. Zbtb14 immunostaining at 3 PM, 11 PM, and 3 AM in the dorsal and ventral hilus and layer VI of the somatosensory cortex. Representative images from 3 PM, 11 PM, and 3 AM time points in the ventral and dorsal hippocampal hilus and the somatosensory cortex. Note the lower expression of Zbtb14 in the ventral hilus at 11 PM—scale bar: 50 µm.

Table 1
The presence of the ZF5 motif (GSGCGCGR; TF: M00716_1) in the promoters of genes downregulated in an in vitro model of epileptiform discharges.

Official Gene Symbol	Full Name	Fold Change	ZF5 Motif
Adamts15	ADAM metallopeptidase with thrombospondin type 1 motif, 15	−5.95	+
Adamts8	ADAM metallopeptidase with thrombospondin type 1 motif, 8	−3.16	+
Bola1	bolA family member 1	−0.95	+
Camkk1	calcium/calmodulin-dependent protein kinase kinase 1	−0.85	+
Drp2	dystrophin-related protein 2	−1.10	−
Emc9	ER membrane protein complex subunit 9	−1.43	+
Galntl6	polypeptide N-acetylgalactosaminyltransferase-like 6	−2.79	−
Grik1	glutamate ionotropic receptor kainate type subunit 1	−3.40	+
Hcrtr1	hypocretin receptor 1	−3.80	+
Ifit1bl	interferon-induced protein with tetratricopeptide repeats 1B-like	−2.92	−
Inha	inhibin subunit alpha	−1.16	+
Kcnab2	potassium voltage-gated channel subfamily A regulatory acct subunit 2 (Kcnab2)	−1.47	+
Lrrc24	leucine-rich repeat containing 24	−0.88	+
Polr3k	RNA polymerase III subunit K	−0.56	+
Ppp1r3e	protein phosphatase 1, regulatory subunit 3E	−1.47	+
RGD1562229	similar to the hypothetical protein FLJ40298	−5.72	+
RT1-DMa	RT1 class II, locus Dma	−1.12	+
Rtl6	retrotransposon Gag like 6	−0.46	+
Rxrg	retinoid X receptor gamma	−2.45	+
Sh3rf3	SH3 domain containing ring finger 3	−1.34	+
Slc7a4	solute carrier family 7, member 4	−1.54	+
Synpr	synaptoporin	−1.71	+
1700030J22Rik	RIKEN cDNA 1700030J22 gene	−1.34	+
AABR07001519.1		−1.39	+

$p_{adj} = 7.233 \times 10^{-4}$

Many of the above genes have essential roles in the brain function. For example, Adamts15 and Adamts8 are metalloproteases that reshape perineuronal nets (Rossier et al., 2015); Kcnab2 is a subunit of voltage-gated potassium channel complexes that play an essential part in neuronal excitability and is a risk factor for epilepsy (Kurosawa et al., 2005; Yee et al., 2022); Synpr is a component of synaptic vesicle membranes and the marker of sprouting of the mossy fiber in the hippocampus (Knaus et al., 1990, Cabrera et al., 2022); Grik1 encodes an ionotropic glutamate receptor subunit known as GluK1 and is involved in synaptic transmission and plasticity (Valbuena et al., 2019); Hcrtr1, hypocretin/orexin receptor 1 can induce neurotransmitter release both post- and pre-synaptically, is known to play a role in the sleep-wake cycle, seizures and anxiety (Scott et al., 2011; Kordi Jaz et al., 2017; Li et al., 2018); Retinoid X receptor gamma (Rxrg) is part of a nuclear receptor family and is activated by retinoic acid supports the survival of dopaminergic neurons (Friling et al., 2009); Polr3k is one of the subunits RNA polymerase III which decreased activity perturbs protein and neurotransmitter shuttling via the ER and affects synaptic plasticity in both axons and dendrites (Lata et al., 2021). The Zbtb14 protein seemingly regulates the genes associated with synaptic activity, transmission, and plasticity.

Our previous transcriptomics data (Debski et al., 2020) from the ventral hippocampus of control and epileptic animals share three differentially expressed genes with the *in vitro* data presented in this paper: Adamts15, 1700030J22Rik, and Inha. Debski et al. (Debski et al., 2020) reported that *in vivo* Adamts15 and 1700030J22Rik did not have circadian oscillations in control animals but gained oscillatory patterns in pilocarpine-treated epileptic animals (Debski et al., 2020). This circadian dynamics change in Adamts15 might result in altered regulatory function on the extracellular matrix of Adamts15 triggered by epilepsy. Conversely, Inha oscillates throughout the circadian cycle in control animals, but this rhythm is abolished in epileptic animals. The overlap of three genes, Adamts15, 1700030J22Rik, and Inha, from two different experimental datasets, strengthens the possibility of the involvement of the Zbtb14 transcription factor in their regulation. This issue requires further studies.

Although epileptic seizures appear as random events, clinical data, patient journals, and basic research have shown that seizures occur more

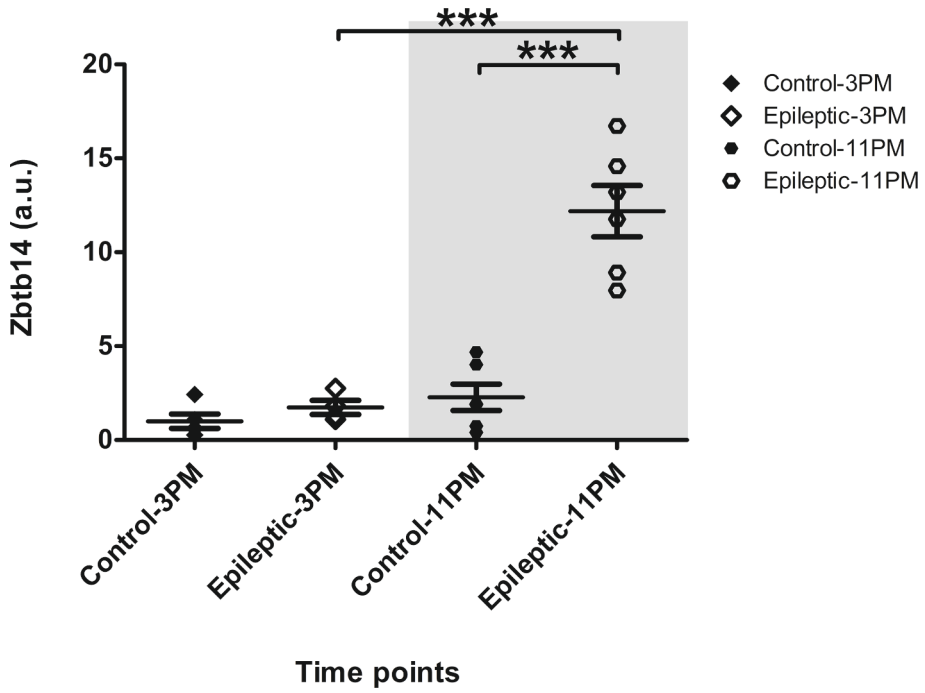

Fig. 5. Zbtb14 protein expression in the hippocampus in pilocarpine-induced epilepsy. The relative ratios of Zbtb14 to β-actin are represented as the mean ± SEM (n = 5 for Control-3 PM, n = 4 for Epileptic-3 PM, and n = 6 for Control- and Epileptic-11 PM; *p < 0.05, **p < 0.01, ***p < 0.001, one-way ANOVA with Bonferroni's multiple comparison post hoc test).

often at certain times over the circadian cycle (Hofstra et al., 2009; Karoly et al., 2021; Zhang et al., 2021; Sun and Wang, 2023). The investigation of cycles from circadian to circannual is becoming an important research topic due to the prospect of chronotherapy – administering drugs when they are most effective. Whether the temporal pattern of seizure rhythmicity stems, at least in part, from proteins like Zbtb14 is an interesting hypothesis to test, as it may provide an attractive novel therapeutic target.

Limitations of the study

In this study, we only used male animals to reduce the complexity of accounting for the female estrous cycle. However, we recognize the need to include female animals in future studies as several epidemiological studies are emphasizing the sexual dimorphism in epilepsy, including the differences in the types of epilepsy females tend to have, seizure threshold, and epileptogenesis (Reddy et al., 2021; Hophing et al., 2022). Changes in cell densities are evaluated using relative measures. Stereological cell counting could not be used due to fresh frozen tissue.

CRediT authorship contribution statement

İlke Güntan: Formal analysis, Investigation, Writing – original draft, Writing – review & editing. **Antoine Ghestem:** Investigation. **Kinga Nazaruk:** Investigation. **Karolina Nizińska:** Investigation. **Maciej Olszewski:** Investigation. **Dorota Nowicka:** Investigation, Supervision, Writing – review & editing. **Christophe Bernard:** Conceptualization, Supervision, Writing – original draft, Writing – review & editing. **Katarzyna Łukasiuk:** Conceptualization, Formal analysis, Funding acquisition, Investigation, Methodology, Supervision, Writing – original draft, Writing – review & editing.

Funding

This work was supported by the Polish National Research Grant 2015/18/M/NZ3/00779 (KL) and the European Union's Horizon 2020 research and innovation programme under the Marie Skłodowska-Curie COFUND grant agreement No 665735 (IG).

The manuscript has been posted as a pre-print at bioRxiv preprint https://doi.org/10.1101/2024.03.07.583828;

Declaration of Competing Interest

The authors declare that they have no known competing financial interests or personal relationships that could have appeared to influence the work reported in this paper.

References

Amaral, D.G., Scharfman, H.E., Lavenex, P., 2007. The dentate gyrus: fundamental neuroanatomical organization (dentate gyrus for dummies). Prog. Brain Res. 163, 3–22.

Baud, M.O., Ghestem, A., Benoliel, J.J., Becker, C., Bernard, C., 2019. Endogenous multidien rhythm of epilepsy in rats. Exp. Neurol. 315, 82–87.

Bernard, C., 2021. Circadian/multidien Molecular Oscillations and Rhythmicity of Epilepsy (MORE). Epilepsia 62 (Suppl. 1), S49–S68.

Bienkowski, M.S., Bowman, I., Song, M.Y., Gou, L., Ard, T., Cotter, K., Zhu, M., Benavidez, N.L., Yamashita, S., Abu-Jaber, J., Azam, S., Lo, D., Foster, N.N., Hintiryan, H., Dong, H.W., 2018. Integration of gene expression and brain-wide connectivity reveals the multiscale organization of mouse hippocampal networks. Nat. Neurosci. 21 (11), 1628–1643.

Bozek, K., Relógio, A., Kielbasa, S.M., Heine, M., Dame, C., Kramer, A., Herzel, H., 2009. Regulation of clock-controlled genes in mammals. PLoS One 4 (3), e4882.

Brancati, G.E., Rawas, C., Ghestem, A., Bernard, C., Ivanov, A.I., 2021. Spatio-temporal heterogeneity in hippocampal metabolism in control and epilepsy conditions. PNAS 118 (11).

Buckmaster, P.S., Reyes, B., Kahn, T., Wyeth, M., 2022. Ventral hippocampal formation is the primary epileptogenic zone in a rat model of temporal lobe epilepsy. J. Neurosci. 42 (39), 7482–7495.

Cabrera, O.H., Useinovic, N., Maksimovic, S., Near, M., Quillinan, N., Todorovic, S.M., Jevtovic-Todorovic, V., 2022. Neonatal ketamine exposure impairs infrapyramidal bundle pruning and causes lasting increase in excitatory synaptic transmission in hippocampal CA3 neurons. Neurobiol. Dis. 175, 105923.

Debski, K., Ceglia, N., Ghestem, A., Ivanov, A., Brancati, G., Broer, S., Bot, A., Muller, J., Schoch, S., Becker, A., Loscher, W., Guye, M., Sassone-Corsi, P., Lukasiuk, K., Baldi, P., Bernard, C., 2020. The circadian dynamics of the hippocampal transcriptome and proteome is altered in experimental temporal lobe epilepsy. Sci. Adv. 6 (41).

Dobin, A., Davis, C.A., Schlesinger, F., Drenkow, J., Zaleski, C., Jha, S., Batut, P., Chaisson, M., Gingeras, T.R., 2013. STAR: ultrafast universal RNA-seq aligner. Bioinformatics 29 (1), 15–21.
Dunn, J.R., Reed, J.E., du Plessis, D.G., Shaw, E.J., Reeves, P., Gee, A.L., Warnke, P., Walker, C., 2006. Expression of ADAMTS-8, a secreted protease with antiangiogenic properties, is downregulated in brain tumours. Br. J. Cancer 94 (8), 1186–1193.
Friling, S., Bergsland, M., Kjellander, S., 2009. Activation of Retinoid X Receptor increases dopamine cell survival in models for Parkinson's disease. BMC Neurosci. 10, 146.
Fujimura, H., Ohsawa, K., Funaba, M., Murata, T., Murata, E., Takahashi, M., Abe, M., Torii, K., 1999. Immunological localization and ontogenetic development of inhibin alpha subunit in rat brain. J. Neuroendocrinol. 11 (3), 157–163.
Grabowska, A., Sas-Nowosielska, H., Wojtas, B., Holm-Kaczmarek, D., Januszewicz, E., Yushkevich, Y., Czaban, I., Trzaskoma, P., Krawczyk, K., Gielniewski, B., Martin-Gonzalez, A., Filipkowski, R.K., Olszynski, K.H., Bernas, T., Szczepankiewicz, A.A., Sliwinska, M.A., Kanhema, T., Bramham, C.R., Bokota, G., Plewczynski, D., Wilczynski, G.M., Magalska, A., 2022. Activation-induced chromatin reorganization in neurons depends on HDAC1 activity. Cell Rep. 38 (7), 110352.
Hastings, M.H., Maywood, E.S., Brancaccio, M., 2018. Generation of circadian rhythms in the suprachiasmatic nucleus. Nat. Rev. Neurosci. 19 (8), 453–469.
Hetman, M., Slomnicki, L.P., Hodges, E.R., Saraswat Ohri, S., Whittemore, S.R., 2022. Role of circadian rhythms in pathogenesis of acute CNS injuries: Insights from experimental studies. Exp. Neurol. 353, 114080.
Hofstra, W.A., Spetgens, W.P., Leijten, F.S., van Rijen, P.C., Gosselaar, P., van der Palen, J., de Weerd, A.W., 2009. Diurnal rhythms in seizures detected by intracranial electrocorticographic monitoring: an observational study. Epilepsy Behav. 14 (4), 617–621.
Hophing, L., Kyriakopoulos, P., Bui, E., 2022. Sex and gender differences in epilepsy. Int. Rev. Neurobiol. 164, 235–276.
Irie, M., Itoh, J., Matsuzawa, A., Ikawa, M., Kiyonari, H., Kihara, M., Suzuki, T., Hiraoka, Y., Ishino, F., Kaneko-Ishino, T., 2022. Retrovirus-derived RTL5 and RTL6 genes are novel constituents of the innate immune system in the eutherian brain. Development 149 (18).
Jiang, Q., Wu, Y., Wang, J., Wu, X., Qin, J., Jiang, Y., 2010. Characterization of developing rat cortical neurons after epileptiform discharges. Int. J. Dev. Neurosci. 28 (6), 455–463.
Karoly, P.J., Rao, V.R., Gregg, N.M., Worrell, G.A., Bernard, C., Cook, M.J., Baud, M.O., 2021. Cycles in epilepsy. Nat. Rev. Neurol. 17 (5), 267–284.
Knaus, P., Marquèze-Pouey, B., Scherer, H., Betz, H., 1990. Synaptoporin, a novel putative channel protein of synaptic vesicles. Neuron 5 (4), 453–462.
Kordi Jaz, E., Moghimi, A., Fereidoni, M., Asadi, S., Shamsizadeh, A., Roohbakhsh, A., 2017. SB-334867, an orexin receptor 1 antagonist, decreased seizure and anxiety in pentylenetetrazol-kindled rats. Fundam. Clin. Pharmacol. 31 (2), 201–207.
Kurosawa, K., Kawame, H., Okamoto, N., Ochiai, Y., Akatsuka, A., Kobayashi, M., Shimohira, M., Mizuno, S., Wada, K., Fukushima, Y., Kawawaki, H., Yamamoto, T., Masuno, M., Imaizumi, K., Kuroki, Y., 2005. Epilepsy and neurological findings in 11 individuals with 1p36 deletion syndrome. Brain Dev. 27 (5), 378–382.
Lane, J.M., Qian, J., Mignot, E., Redline, S., Scheer, F.A.J.L., Saxena, R., 2023. Genetics of circadian rhythms and sleep in human health and disease. Nat. Rev. Genet. 24 (1), 4–20.
Lata, E., Choquet, K., Sagliocco, F., Brais, B., Bernard, G., Teichmann, M., 2021. RNA Polymerase III Subunit Mutations in Genetic Diseases. Front. Mol. Biosci. 8, 696438.
Lee, K.H., Kwak, Y.D., Kim, D.H., Chang, M.Y., Lee, Y.S., 2004. Human zinc finger protein 161, a novel transcriptional activator of the dopamine transporter. Biochem. Biophys. Res. Commun. 313 (4), 969–976.
Li, S., Franken, P., Vassalli, A., 2018. Bidirectional and context-dependent changes in theta and gamma oscillatory brain activity in noradrenergic cell-specific Hypocretin/Orexin receptor 1-KO mice. Sci. Rep. 8 (1), 15474.
Li, P., Fu, X., Smith, N.A., Ziobro, J., Curiel, J., Tenga, M.J., Martin, B., Freedman, S., Cea-Del Rio, C.A., Oboti, L., Tsuchida, T.N., Oluigbo, C., Yaun, A., Magge, S.N., O'Neill, B., Kao, A., Zelleke, T.G., Depositario-Cabacar, D.T., Ghimbovschi, S., Knoblach, S., Ho, C.Y., Corbin, J.G., Goodkin, H.P., Vicini, S., Huntsman, M.M., Gaillard, W.D., Valdez, G., Liu, J.S., 2017. Loss of CLOCK Results in Dysfunction of Brain Circuits Underlying Focal Epilepsy. Neuron 96 (2), 387–401.e386.
Liao, Y., Smyth, G.K., Shi, W., 2014. featureCounts: an efficient general purpose program for assigning sequence reads to genomic features. Bioinformatics 30 (7), 923–930.
Lothmann, K., Deitersen, J., Zilles, K., Amunts, K., Herold, C., 2021. New boundaries and dissociation of the mouse hippocampus along the dorsal-ventral axis based on glutamatergic, GABAergic and catecholaminergic receptor densities. Hippocampus 31 (1), 56–78.
Love, M.I., Huber, W., Anders, S., 2014. Moderated estimation of fold change and dispersion for RNA-seq data with DESeq2. Genome Biol. 15 (12), 550.
Markov, D., Goldman, M., 2006. Normal sleep and circadian rhythms: neurobiologic mechanisms underlying sleep and wakefulness. Psychiatr. Clin. North Am. 29 (4), 841–853 abstract vii.
Matos, H.C., Koike, B.D.V., Pereira, W.D.S., de Andrade, T.G., Castro, O.W., Duzzioni, M., Kodali, M., Leite, J.P., Shetty, A.K., Gitaí, D.L.G., 2018. Rhythms of core clock genes and spontaneous locomotor activity in post-. Front. Neurol. 9, 632.
McCullough, K.M., Daskalakis, N.P., Gafford, G., Morrison, F.G., Ressler, K.J., 2018. Cell-type-specific interrogation of CeA Drd2 neurons to identify targets for pharmacological modulation of fear extinction. Transl. Psychiatry 8 (1), 164.
Numoto, M., Niwa, O., Kaplan, J., Wong, K.K., Merrell, K., Kamiya, K., Yanagihara, K., Calame, K., 1993. Transcriptional repressor ZF5 identifies a new conserved domain in zinc finger proteins. Nucleic Acids Res. 21 (16), 3767–3775.
Nylén, C., Aoi, W., Abdelmoez, A.M., Lassiter, D.G., Lundell, L.S., Wallberg-Henriksson, H., Näslund, E., Pillon, N.J., Krook, A., 2018. IL6 and LIF mRNA expression in skeletal muscle is regulated by AMPK and the transcription factors NFYC, ZBTB14, and SP1. Am. J. Phys. Endocrinol. Metab. 315 (5), E995–E1004.
Obata, T., Yanagidani, A., Yokoro, K., Numoto, M., Yamamoto, S., 1999. Analysis of the consensus binding sequence and the DNA-binding domain of ZF5. Biochem. Biophys. Res. Commun. 255 (2), 528–534.
O'Leary, O.F., Cryan, J.F., 2014. A ventral view on antidepressant action: roles for adult hippocampal neurogenesis along the dorsoventral axis. Trends Pharmacol. Sci. 35 (12), 675–687.
Orlov, S.V., Kuteykin-Teplyakov, K.B., Ignatovich, I.A., Dizhe, E.B., Mirgorodskaya, O.A., Grishin, A.V., Guzhova, O.B., Prokhortchouk, E.B., Guliy, P.V., Perevozchikov, A.P., 2007. Novel repressor of the human FMR1 gene - identification of p56 human (GCC)(n)-binding protein as a Krüppel-like transcription factor ZF5. FEBS J. 274 (18), 4848–4862.
Quigg, M., Straume, M., Menaker, M., Bertram, E.H., 1998. Temporal distribution of partial seizures: comparison of an animal model with human partial epilepsy. Ann. Neurol. 43 (6), 748–755.
Reddy, D.S., Thompson, W., Calderara, G., 2021. Molecular mechanisms of sex differences in epilepsy and seizure susceptibility in chemical, genetic and acquired epileptogenesis. Neurosci. Lett. 750, 135753.
Rijo-Ferreira, F., Takahashi, J.S., 2019. Genomics of circadian rhythms in health and disease. Genome Med. 11 (1), 82.
Rossier, J., Bernard, A., Cabungcal, J.H., Perrenoud, Q., Savoye, A., Gallopin, T., Hawrylycz, M., Cuénod, M., Do, K., Urban, A., Lein, E.S., 2015. Cortical fast-spiking parvalbumin interneurons enwrapped in the perineuronal net express the metallopeptidases Adamts8, Adamts15 and Neprilysin. Mol. Psychiatry 20 (2), 154–161.
Schurhoff, N., Toborek, M., 2023. Circadian rhythms in the blood-brain barrier: impact on neurological disorders and stress responses. Mol. Brain 16 (1), 5.
Scott, M.M., Marcus, J.N., Pettersen, A., Birnbaum, S.G., Mochizuki, T., Scammell, T.E., Nestler, E.J., Elmquist, J.K., Lutter, M., 2011. Hcrtr1 and 2 signaling differentially regulates depression-like behaviors. Behav. Brain Res. 222 (2), 289–294.
Sun, S., Wang, H., 2023. Reprogramming the circadian dynamics of epileptic genes in mouse temporal lobe epilepsy. Int. J. Mol. Sci. 24 (7).
Tamanini, F., Yagita, K., Okamura, H., van der Horst, G.T., 2005. Nucleocytoplasmic shuttling of clock proteins. Methods Enzymol. 393, 418–435.
Tamaru, T., Isojima, Y., van der Horst, G.T., Takei, K., Nagai, K., Takamatsu, K., 2003. Nucleocytoplasmic shuttling and phosphorylation of BMAL1 are regulated by circadian clock in cultured fibroblasts. Genes Cells 8 (12), 973–983.
Valbuena, S., García, Á., Mazier, W., Paternain, A.V., Lerma, J., 2019. Unbalanced dendritic inhibition of CA1 neurons drives spatial-memory deficits in the Ts2Cje Down syndrome model. Nat. Commun. 10 (1), 4991.
Wyeth, M., Nagendran, M., Buckmaster, P.S., 2020. Ictal onset sites and γ-aminobutyric acidergic neuron loss in epileptic pilocarpine-treated rats. Epilepsia 61 (5), 856–867.
Xu, S.Y., Wu, Y.M., Ji, Z., Gao, X.Y., Pan, S.Y., 2012. A modified technique for culturing primary fetal rat cortical neurons. J. Biomed. Biotechnol. 2012, 803930.
Yee, J.X., Rastani, A., Soden, M.E., 2022. The potassium channel auxiliary subunit Kvβ2. J. Neurophysiol. 128 (1), 62–72.
Yokoro, K., Yanagidani, A., Obata, T., Yamamoto, S., Numoto, M., 1998. Genomic cloning and characterization of the mouse POZ/zinc-finger protein ZF5. Biochem. Biophys. Res. Commun. 246 (3), 668–674.
Zhang, T., Yu, F., Xu, H., Chen, M., Chen, X., Guo, L., Zhou, C., Xu, Y., Wang, F., Yu, J., Wu, B., 2021. Dysregulation of REV-ERBα impairs GABAergic function and promotes epileptic seizures in preclinical models. Nat. Commun. 12 (1), 1216.